Available online at www.sciencedirect.com

SCIENCE DIRECT®

Journal of Catalysis 224 (2004) 236–242

JOURNAL OF CATALYSIS

www.elsevier.com/locate/jcat

PtRuRhNi nanoparticle electrocatalyst for methanol electrooxidation in direct methanol fuel cell

Kyung-Won Park,[a] Jong-Ho Choi,[b] Seol-Ah Lee,[c] Chanho Pak,[c] Hyuck Chang,[c]
and Yung-Eun Sung[a,*]

[a] *School of Chemical Engineering & Research Center for Energy Conversion and Storage, Seoul National University, Seoul 151-744, South Korea*
[b] *Department of Materials Science and Engineering, Kwangju Institute of Science and Technology, Kwangju 500-712, South Korea*
[c] *Fuel Cell Project Team and Materials and Devices Laboratory, Samsung Advanced Institute of Technology, PO Box 111, Suwon 440-600, South Korea*

Received 2 October 2003; revised 30 January 2004; accepted 4 February 2004

Abstract

The enhanced catalytic activity of PtRuRhNi was examined in relation to the oxidation of methanol in a direct methanol fuel cell. As evidenced by transmission electron microscopy and X-ray diffraction analysis, the synthesized PtRuRhNi appeared to be a well-synthesized Pt-based alloy nanoparticle. The catalytic activity of PtRuRhNi alloy electrocatalyst was superior to that of PtRu, from the standpoint of its high oxidation current, power density, and better stability in the electrochemical half- and single-cell measurements. Through X-ray absorption near edge structure and X-ray photoelectron spectroscopy, it was found that Pt and Ru in the PtRuRhNi are present in electronic and chemical states that are favorable to methanol electrooxidation. The dominant existence of Pt and Ru metallic states on the catalyst was essential for its high surface activity with respect to methanol electrooxidation. However, the catalytic enhancement of PtRuRhNi due to the chemical states of Rh/Ni was considered and examined.

Keywords: PtRuRhNi; Electrocatalyst; Methanol oxidation; DMFC

1. Introduction

In low-temperature fuel cells, e.g., polymer electrolyte membrane fuel cells using hydrogen or methanol as a fuel, platinum-based alloy nanoparticles have been extensively examined in terms of the oxidation of hydrogen or methanol for use as an anode in fuel cells. Direct oxidation methanol fuel cell (DMFC), which uses methanol directly as fuel, has been a subject of intense study because of its numerous advantages [1–6]. The excellent catalytic activity of platinum with respect to methanol oxidation at low temperatures makes this metal electrocatalyst ideal for use as an anode in DMFCs. However, since the pure platinum is readily poisoned by CO species, a by-product produced during methanol oxidation, considerable effort has been made to design and synthesize Pt-based alloy catalysts by alloying platinum with other elements to enhance its catalytic activity by eliminating or inhibiting the CO-poisoning effect. An important process to overcome CO-poisoning effect and improve methanol oxidation is as follows (bifunctional effect): the CO-poisoned platinum can be freshened by means of the reaction of surface CO with oxygen species adsorbed on a water-activating element such as ruthenium to oxidize CO into CO_2 [7,8]. In addition, it has been reported that enhanced methanol oxidation in Pt-based nanoparticles that have been alloyed with a transition metal such as Ni, which has a lower electronegativity than Pt, can be attributed to a change in the electronic properties of Pt (electronic effect) [9–12]. The electron donation of Ni to Pt would result in a change in the electronic properties of the Pt $4f$ peaks. The findings herein indicate that such modified electronic properties of platinum improve the electrocatalytic activity of Pt-based alloys. The shift in d electron density from Ni to Pt would lower the density of state (DOS) on the Fermi level and reduce the Pt–CO bond energy. Accordingly, the best candidate for methanol oxidation in DMFCs would be designed by considering appropriate materials that affect methanol electrooxidation based on either the bifunctional

---

* Corresponding author.
E-mail address: ysung@snu.ac.kr (Y.-E. Sung).

0021-9517/$ – see front matter © 2004 Published by Elsevier Inc.
doi:10.1016/j.jcat.2004.02.010

effect or the electronic effect [13]. In this paper, the preparation of PtRuRhNi multimetallic nanoparticle by the borohydride reduction method for enhanced methanol electrooxidation in a DMFC is desired. The Pt-based nanoparticles were characterized by transmission electron microscopy (TEM), X-ray diffraction (XRD), X-ray absorption near edge structure (XANES), X-ray photoelectron spectroscopy (XPS), and electrochemical half- and single-cell measurements.

2. Experimental

The PtRuRhNi (50:40:5:5) electrocatalyst was prepared using a $NaBH_4$ reduction method, which is frequently used to prepare high-surface-area Pt-based alloy electrocatalysts [14,15], at room temperature, combined with freeze-drying. $H_2PtCl_6 \cdot xH_2O$ (Aldrich Chem. Co.), $RuCl_3 \cdot xH_2O$ (Aldrich Chem. Co.), $NiCl_2 \cdot 6H_2O$ (Aldrich Chem. Co.), and $RhCl_3 \cdot xH_2O$ (Aldrich Chem. Co.) were used as metal salts and were dissolved completely in Millipore water (18 MΩ cm). After several hours, the salts were reduced by quickly pouring the entire volume of a concentrated $NaBH_4$ solution (0.1 g of $NaBH_4$ per ml of water) under high-speed stirring to produce the alloy catalyst via the complete reduction of the metal salts. The resulting material was washed with deionized water several times and dried by freeze-drying without any heat treatment.

A transmission electron microscopy (TEM) investigation was carried out using a Phillips CM20T/STEM electron microscope at an accelerating voltage of 200 kV. Specimens were prepared by ultrasonically suspending the particles in deionized water. Drops of this suspension were deposited onto a standard Cu grid covered with carbon film (200 mesh) and allowed to dry before being inserted into the microscope. X-ray absorption near edge (XANES) spectra of the Pt L_{III} and Ru K edges were recorded ex situ in the transmission mode at beam-line 7C of the Pohang Accelerator Laboratory (PAL) using a Si (311) double-crystal monochromator. The analysis of X-ray absorption spectra was performed by the standard procedure using the WINXAS v. 1.3 software program. In the XANES analysis, the first inflection points of all samples were adjusted and aligned to the edge energies of the Pt foil and Ru powder. To analyze the surface chemical states of the samples, XPS analysis was carried out using a VG Scientific (ESCALAB 200R) photoelectron spectrometer. The X-ray source was Al K_α at 1486.6 eV operating at 15 kV and 300 W. The base pressure of the system was 10^{-10} Torr. The XPS core-level spectra were fitted to the Doniach-Sunjic lineshape convoluted by a Gaussian contribution taking into account the spectrometer resolution. Both ends of the baseline were set sufficiently far apart so as not to distort the shape of spectra, including the tails. Small variations in the range of the baseline had no effect on the relative amount of fitted species (less than 1%). As reported previously, all binding energies were calibrated by referencing Au $4f_{7/2}$ (84.0 eV) and Cu $2p_{3/2}$ (932.66 eV) of sputter-cleaned Au and Cu.

Electrochemical measurements were made using a three-electrode cell at 25 °C. Pt gauze and Ag/AgCl (in saturated KCl) were used as the counter and reference electrodes, respectively. All potentials are reported with respect to a normal hydrogen electrode (NHE). The carbon electrode as the working electrode was polished with 1, 0.3, and 0.05 µm Al_2O_3 paste and washed ultrasonically in Millipore water (18 MΩ cm). The working electrode was brushed with catalyst ink as described previously [16]. Solutions of 0.5 M H_2SO_4 and 2.0 M CH_3OH in 0.5 M H_2SO_4 were stirred constantly and purged with nitrogen gas. All chemicals used were of analytical grade. Electrochemical experiments were performed with an AUTOLAB instrument from Eco Chemie. To identify the properties of the Pt-based catalyst and to evaluate the catalytic activity of the catalysts, cyclic voltammetry (CV) and I–V characteristic curves for the electrooxidation of methanol were examined at 25 °C.

Cell performance was evaluated using a DMFC single cell with a 2 cm^2 cross-sectional area and measured with a potentiometer which recorded the cell potential from the circuit voltage under constant current conditions [17]. The catalysts used at the anode and cathode were applied on carbon paper (Toray) by a brushing method [16,17]. The loading on all electrodes was 5 mg/cm^2. The solid electrolyte was a Nafion 117 (DuPpont), which was pretreated with H_2O_2 and H_2SO_4 solutions. A membrane electrode assembly (MEA) was prepared by hot pressing (110 °C, 55 atm) for 3 min. A 2 M methanol solution at the anode was supplied by a Masterflex liquid micropump at 1 ml/min while the cathode was fed with dry O_2 at a rate of 500 ml/min by means of a flowmeter. A stability test of the catalysts was evaluated and measured with a potentiometer, which recorded the current density under constant voltage conditions.

3. Results and discussion

The size and dispersion of PtRuRhNi prepared for methanol electrooxidation in DMFC are shown in Fig. 1. In Fig. 1a, the electrocatalyst shows an approximate size of 4.5 nm, slightly larger than that of a commercial PtRu catalyst (Johnson Matthey Co.). The circular shape of the patterns in the inset of Fig. 1a indicates that these nanosized particles are formed from polycrystalline powder. The crystalline plane of the PtRuRhNi nanoparticles can be observed in a high-resolution TEM image, as shown in Fig. 1b. The d spacing of the (111) plane in the PtRuRhNi nanoparticle is reduced to $d_{111} \sim 0.224$ nm, compared to $d_{111} \sim 0.228$ nm in the pure Pt, indicative of good alloy formation between Pt and other elements such as Ru, Ni, and Rh [6,18]. The intended ratio (50:40:5:5) of PtRuNiRh is in relatively good agreement with the composition measured by EDX analysis of a multimetallic nanoparticle. As shown in Fig. 2, the XRD

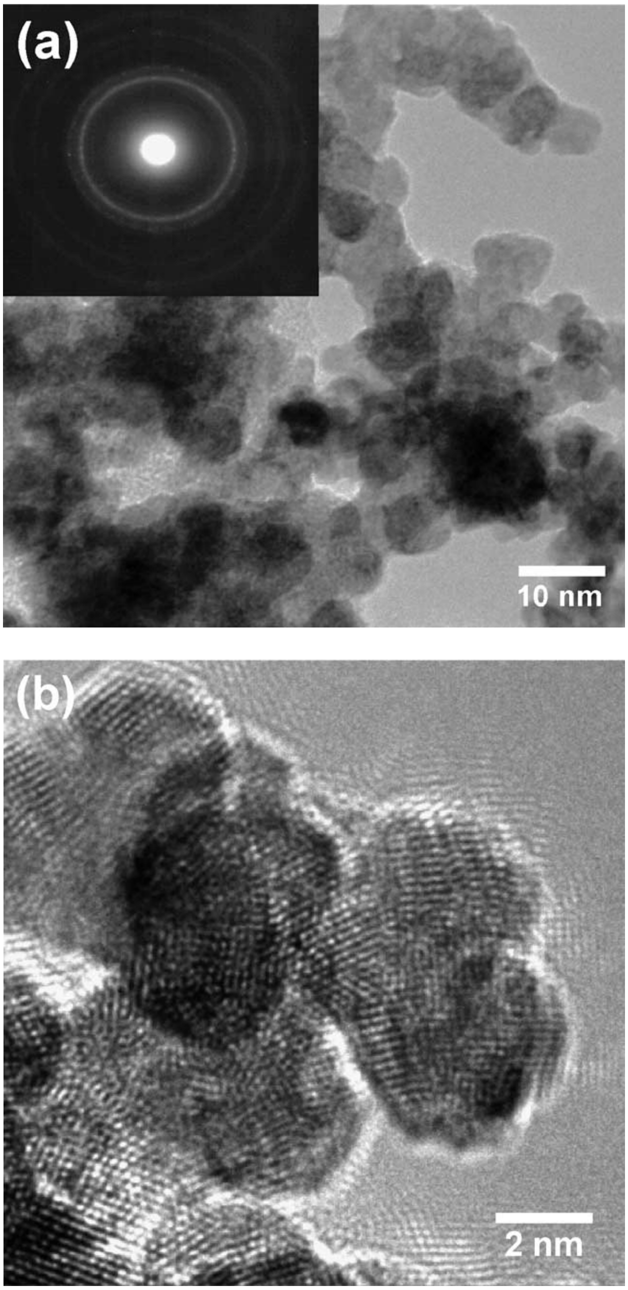

Fig. 1. (a) Transmission electron microscopy (TEM) (insert: transmission electron diffraction (TED) pattern) and (b) high-resolution TEM image of PtRuRhNi (50:40:5:5).

analyses clearly demonstrate the characteristic peaks of the Pt fcc structure. In Fig. 2, no peaks for the fcc of Ni and Rh or the hcp of Ru metals or oxides/hydroxides are evident. The 2θ of the (111) peak for PtRu (50:50) and PtRuRhNi (50:40:5:5), which have angle shifts higher than 39.83 of pure Pt, are 40.29 and 40.20, respectively. The higher angle shifts of the Pt peaks are consistent with Pt-based alloy formation with other elements such as Ru, Rh, and Ni with atomic sizes smaller than Pt. In the XRD peak analysis, the average size of the particle is about 3–4 nm, as calculated using the Debye–Scherrer equation, which is in good agreement with that observed by TEM analysis [18].

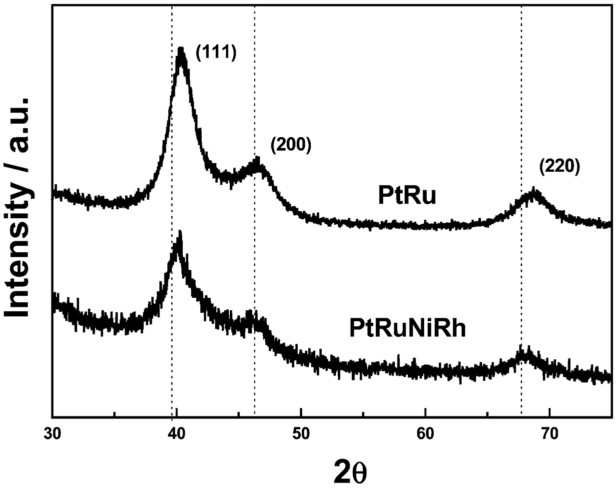

Fig. 2. X-ray diffraction (XRD) patterns of PtRuRhNi (50:40:5:5) and PtRu (50:50).

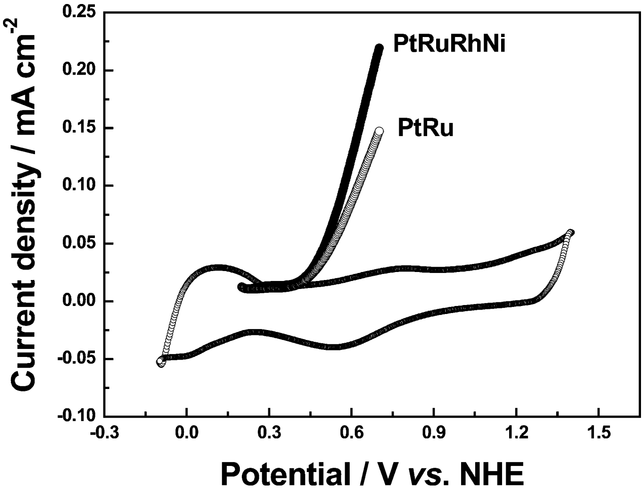

Fig. 3. Potential–current plot for PtRuRhNi (50:40:5:5) in 0.5 M H_2SO_4, and PtRuRhNi (50:40:5:5) and PtRu (50:50) with respect to methanol oxidation in 2.0 M $CH_3OH + 0.5$ M H_2SO_4.

The electrochemical properties of Pt-based nanoparticles were analyzed in 0.5 M H_2SO_4 and 2.0 M CH_3OH in 0.5 M H_2SO_4 using voltammetry. A cyclic voltammogram (CV) of the nanoparticle in 0.5 M H_2SO_4 at room temperature was obtained during scanning between 0.0 to 1.4 V vs NHE with the scan rate of 50 mV/s, as shown in Fig. 3. The electrochemical characteristic curve of PtRuRhNi (50:40:5:5) in 0.5 M H_2SO_4 is indicative of the Pt-based properties, that is, peaks for the adsorption/desorption of hydrogen and preoxidation/reduction. In addition, the methanol oxidation current was measured on PtRuRhNi (50:40:5:5) and PtRu (50:50) in 2.0 M CH_3OH/0.5 M H_2SO_4 at room temperature. Theoretically, methanol oxidation may proceed at 0.04 V vs NHE. Therefore, the lower onset potential provides clear evidence for the superior electrocatalytic activity of this preparation for methanol electrooxidation. The lower onset potential of 0.255 V vs NHE of PtRuRhNi (50:40:5:5), compared to that of 0.265 for PtRu (50:50), indicates its superior elec-

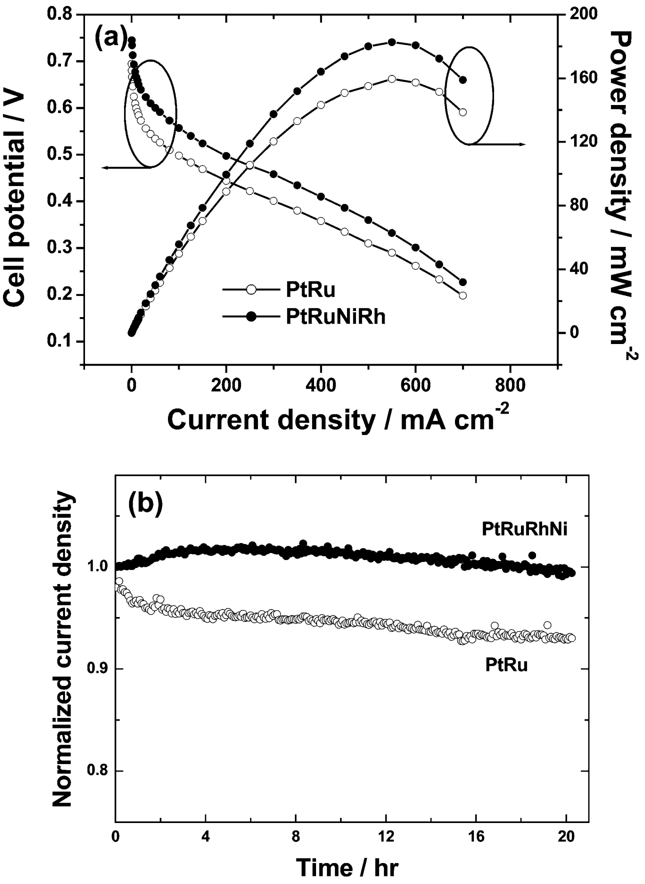

Fig. 4. (a) DMFC unit cell performance using PtRuRhNi (50:40:5:5) and PtRu (50:50) as an anode at 70 °C and (b) plot of normalized current density vs time under a constant applied cell voltage of 0.5 V.

trocatalytic activity. In addition, the PtRuRhNi (50:40:5:5) alloy electrocatalyst showed a higher current density than PtRu (50:50), that is, superior catalytic activity. The value for PtRuRhNi (50:40:5:5) of 16.1 µA/cm^2 at 0.4 V, near the kinetically controlled potential in the methanol reaction, exceeds the value of 13.6 µA/cm^2 for PtRu (50:50).

The significant goal of Pt-based alloy electrocatalysts is their application to the electrodes in actual DMFC systems consisting of a solid-state polymer membrane and electrodes. It is well known that catalysts are the key factors in the performance of fuel cells at low temperature, and a comparison of DMFC performance at relatively low temperatures is the most practical and powerful way of evaluating the activity of a catalyst. A DMFC unit cell measurement was carried out using the Pt-based alloy electrocatalysts as the anode, as shown in the polarization curves at 70 °C in Fig. 4. The open circuit voltages (OCVs) of PtRu (50:50) and PtRuRhNi (50:40:5:5) are $\sim$ 0.70 and $\sim$ 0.74 V, respectively, and the order of OCV is exactly the same as the onset potentials measured in the electrochemical cell. This indicates that the PtRuRhNi shows considerably higher catalytic activity for methanol electrooxidation than PtRu alloy catalysts. At 0.6 V, the activation polarization regime dominantly affected by the activity of the catalyst, the current density (41.6 mA/cm^2) of PtRuRhNi is several times higher than that of PtRu (8.2 mA/cm^2). In addition, the maximum power densities for PtRuRhNi and PtRu are 180 and 160 mW/cm^2, respectively. Such improved activity of the PtRuRhNi indicates that the use of the PtRuRhNi can lead to a substantial reduction in catalyst by several tens of percent in the fuel cell. In the performance of fuel cells, it is clear that the durability of the electrode is significant for practical applications. Accordingly, current density vs time at the applied operating voltage was obtained to compare the stability (or durability) of the electrodes in the DMFC unit cell system. Fig. 4b shows the normalized current density, the ratio of the measured value of the initial value, of PtRuRhNi (50:40:5:5) and PtRu (50:50) at a constant cell voltage. Although the current density of PtRu gradually decreased from the initial state, that of PtRuRhNi remained constant for 21 h. PtRuRhNi maintains its stable catalytic activity, as evidenced by measurement of the current density vs time at the applied operating voltage. Accordingly, we conclude that PtRuRhNi is a highly promising electrocatalyst for fuel cells. It is certain that the outstanding stability of cell performance using PtRuRhNi as an anode would result from superior catalytic durability of PtRuRhNi vis-à-vis PtRu. However, since the issue of the durability of the electrocatalyst is critical, a more intensive study needs to be done and the such investigations are currently underway. The excellent catalytic activity of PtRuRhNi for methanol electrooxidation both in an electrochemical cell and in a single cell is considered to be due to the modified electronic and chemical properties of the elements such as Pt, Ru, Rh, and Ni, which facilitate catalytic reactions.

Fig. 5a shows XANES spectra at the Pt L_{III} edge of Pt foil, PtRu (50:50), and PtRuRhNi (50:40:5:5) catalysts. The white line is the large peak appearing just after the absorption edge. This can be attributed to the electron transition from core $2p$ electrons to unoccupied $5d$ states. Thus, the area of the white line is related to the electron density of the valence state of Pt atoms [19–22]. The increase in d-band vacancies would lead to an increased back donation of CO as a by-product during the methanol oxidation process and, as a result, the strong bond strength between Pt and CO. The white line area of the commercial PtRu electrocatalyst was larger than that of the Pt foil, indicating that the d vacancy of Pt atoms in the PtRu is increased by Ru atoms. The quaternary catalyst showed a decrease in the area of the white line, indicating the Pt in the PtRuRhNi is more metallic than that in the PtRu. Accordingly, methanol electrooxidation by PtRuRhNi would be superior to that of the PtRu. However, enhanced catalytic activity by modified electronic and chemical properties in Pt-based alloy electrocatalysts will be discussed with additional and supplementary information such as XPS analysis. Fig. 5b shows XANES spectra of the catalysts and Ru powder at the Ru K edge. The difference between PtRu and PtRuRhNi is clearer in these spectra. The XANES for PtRuRhNi is similar to that of Ru powder; however, that of PtRu is very different and deviated from the

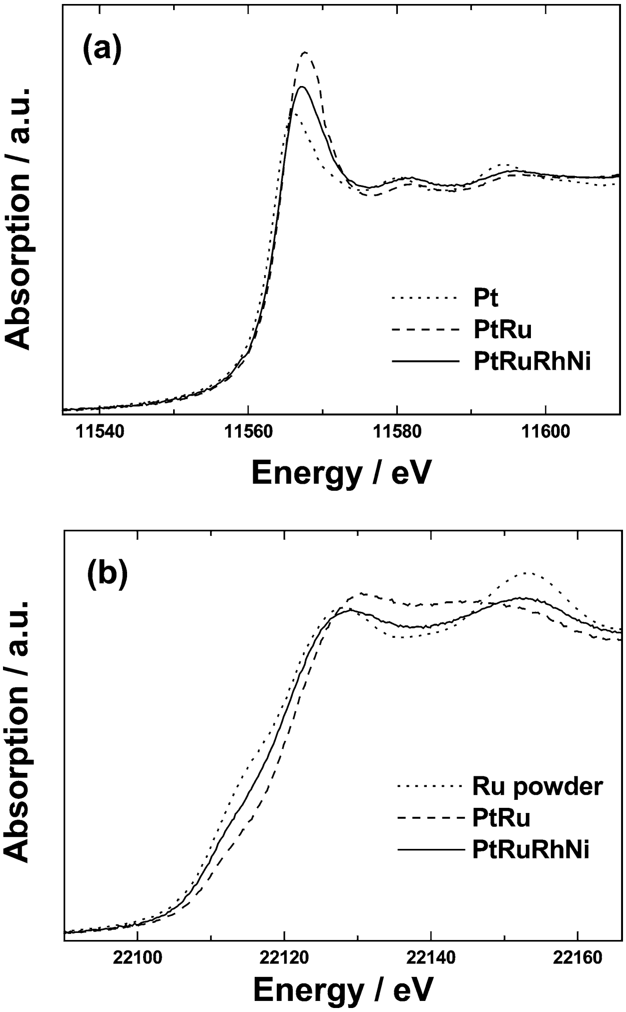

Fig. 5. XANES spectra at (a) Pt L_{III} edge of Pt foil, PtRu (50:50), and PtRuRhNi (50:40:5:5) catalysts and (b) at Ru K edge of the catalysts and Ru powder.

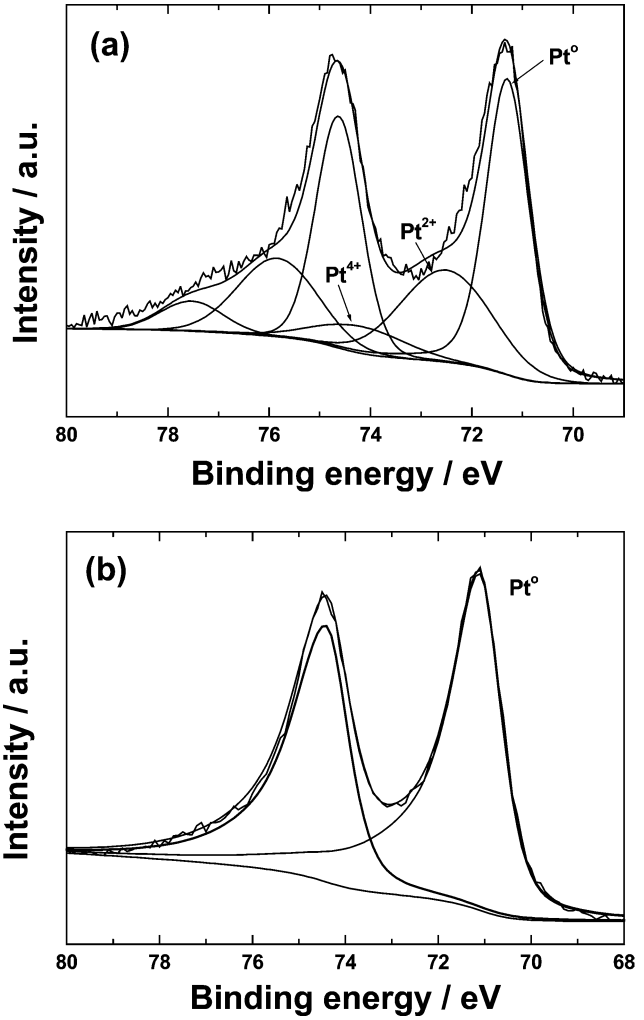

Fig. 6. Pt $4f$ X-ray photoelectron spectra for (a) PtRu (50:50) and (b) PtRuRhNi (50:40:5:5).

Ru metallic state. Recently, Viswanathan et al. reported that PtRu catalysts before and after electrochemical reaction contained a portion of RuO_2 [23]. They also suggested from in situ XANES measurement that the active catalytic component is a metallic PtRu alloy. It has been suggested that the Ru in the PtRuRhNi has a dominant metallic property even when exposed to air. This can be attributed to the high activity and the lower deactivation in methanol electrooxidation than the PtRu alloy electrocatalyst. Thus, it would be expected to increase the performance of DMFC. Further XAS study using ruthenium oxide as a reference will be needed to confirm the results. However, in general, XANES analysis is well known as a bulk technique and, thus, can be combined with surface characterization such as XPS analysis to describe the surface phenomenon related to (electro)catalysis.

For PtRu (50:50) and PtRuRhNi (50:40:5:5), the Pt $4f$ spectra are shown in Fig. 6. The Pt $4f_{7/2}$ and $4f_{5/2}$ lines appear at ~ 71 and ~ 74 eV, respectively, with a theoretical ratio of peak areas of 4 to 3. Small portions of platinum oxides are present in PtRu as indicated by the peaks for Pt^{2+} and Pt^{4+} at 73.8 and 74.6 eV, respectively, while a comparison of the binding energies indicates that Pt is present in the zero-valent metallic state in PtRuRhNi alloy nanoparticles. The surface metallic state of platinum (Pt^0) would provide more suitable sites for methanol electrooxidation than $Pt^{II}O$ or $Pt^{IV}O_2$. Hence, the surface metallic state of Pt on a Pt-based catalyst is essential for high surface activity with respect to methanol electrooxidation. In the case of PtRuRhNi and PtRu, the Ru surface chemical states are shown in Fig. 7. Metallic ruthenium appears as a spin-orbit doublet at 279.9 eV (Ru $3d_{5/2}$) and 284.1 eV (Ru $3d_{3/2}$) with an area ratio of 1.5. RuO_2 was characterized using the $3d_{5/2}$ and $3d_{3/2}$ peaks at 281.2 and 285.4 eV, respectively. Additional Ru peaks were found at 282.7 and 286.9 eV, indicating the formation of a second Ru oxide, RuO_3. It should be noted that metallic ruthenium of 64% in the PtRuRhNi is the dominant state for Ru compared to metallic Ru of 30% and dominant oxidative states in the PtRu. It is probable that the difference in the dominant surface chemical state would result from the method used in the synthesis of the electrocatalysts. The borohydride reduction method

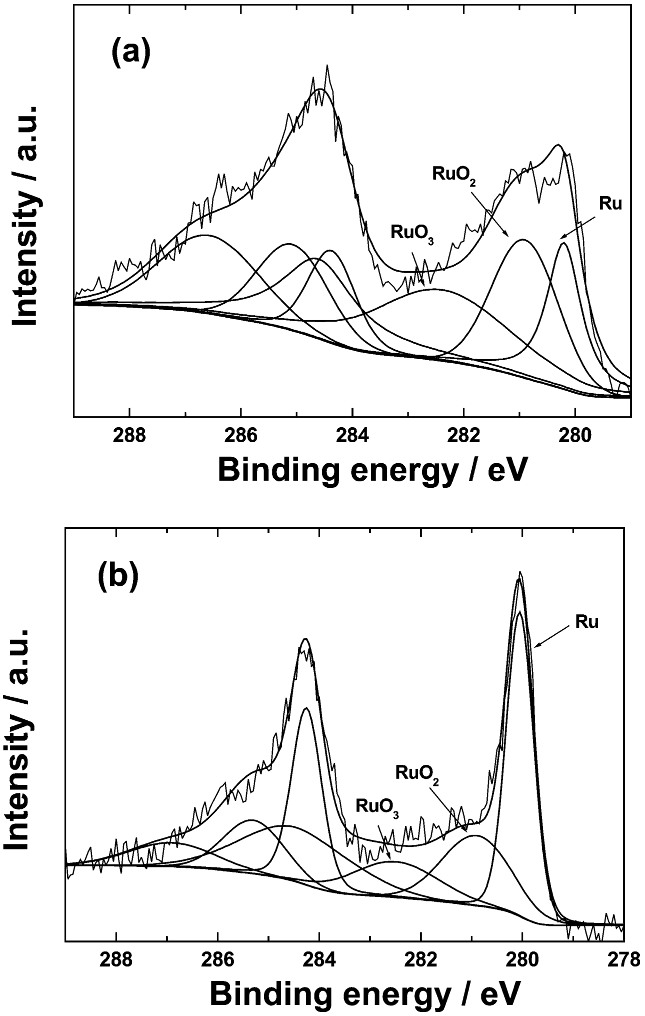

Fig. 7. Ru 3*d* X-ray photoelectron spectra for (a) PtRu (50:50) and (b) PtRu-RhNi (50:40:5:5).

combined with the freeze-drying procedure instead of heat treatment resulted in producing highly dispersed catalysts in pure metallic surface states, even compared to those obtained by a typical borohydride reduction method as well as other methods. Another possible interpretation for the dominant Ru metallic state in PtRuRhNi is that an element such as Ni could be sacrificially oxidized instead of Ru. However, the origin of the dominant surface chemical state in this novel catalyst needs to be considered in further studies. As already observed in the XANES analysis, the Ru in the PtRuRhNi has a dominant metallic property compared to that in PtRu. According to the bifunctional effect, oxophilic Ru sites covered by RuOH are the source of oxygen required for surface CO removal and, as a result, Ru-modified electrocatalysts for methanol electrooxidation have excellent catalytic activity [24–26]. It is likely that the Ru metallic state would play a key role as an oxygen source to oxidize CO [8,27]. Accordingly, the PtRuRhNi with a dominant pure Ru metallic property shows improved methanol electrooxidation compared to PtRu with a dominant Ru oxidative property. However, in the case of PtRuRhNi, which consists of multimetallic elements, the contribution of Rh and Ni to methanol electrooxidation due to the electrochemical and chemical properties of Rh and Ni should be carefully and intensively investigated.

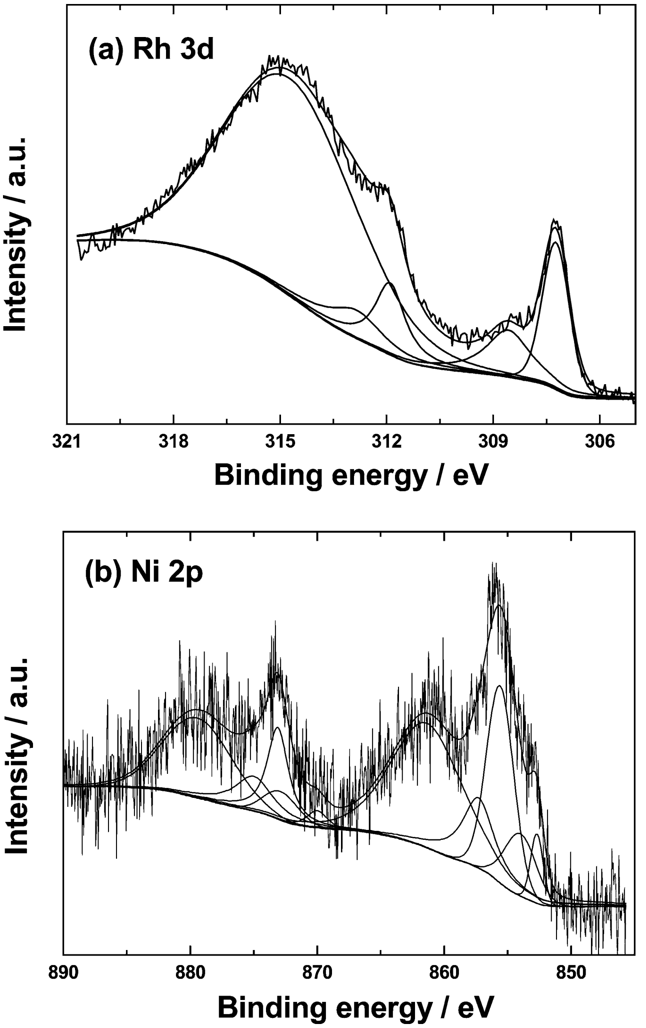

Fig. 8. (a) Rh 3*d* and (b) Ni 2*p* X-ray photoelectron spectra of PtRuRhNi (50:40:5:5).

As shown in Figs. 8a and 8b, the Rh in the catalyst consists of 58.6% metallic Rh and 41.4% Rh_2O_3 while the Ni additive is comprised of various surface chemical states, including 7.4% metallic Ni, 16.6% NiO, 46.2% $Ni(OH)_2$, and 29.8% NiOOH. Such metallic and oxidative states of Rh and Ni in the PtRuRhNi would serve as oxophilic sites for the source of oxygen required for the surface removal of CO. As pointed out above, Ni (hydro)oxides on the PtNi and PtRuNi nanoparticles could promote methanol oxidation via a surface redox process [11]. In addition, it has recently been reported that nickel or nickel hydroxides acting as a catalyst, and not as a promoter or supporter, are capable of oxidizing methanol [28–30]. While contribution of catalytic activities of Rh and Ni to the enhanced methanol electrooxidation in the PtRuRhNi are quite tempting, we also pointed out above that the structural, chemical, and electronic properties of Pt, Ru, Rh, and Ni in the novel electrocatalyst could promote electrochemical properties favorable for methanol oxidation. The balance between these contributions to the enhancement of catalytic properties of the novel electrocatalyst will need to be established in further studies.

4. Conclusions

Methanol electrooxidation by a PtRuRhNi (50:40:5:5) alloy electrocatalyst consisting of multimetallic elements was investigated and the findings compared to that of conventional type PtRu (50:50). The PtRuRhNi showed high oxidation current, power density, and excellent long-term stability in electrochemical half- and single-cell measurements. The PtRuRhNi catalyst was determined to be a Pt-based alloy nanostructure by means of HRTEM and XRD analysis, that is, well-defined mixture with Pt and other metallic elements such as Ru, Rh, and Ni. The electronic and chemical properties of the elements need to be further characterized in relation to this enhanced catalytic activity. In particular, the dominant metallic states of the Pt and Ru in the PtRuRhNi as the electrocatalyst essential for high surface activity of methanol electrooxidation were observed by XANES and XPS analysis. In addition, the PtRuRhNi appears to enhance methanol electrooxidation because of the chemical states of Rh and Ni. However, compared to the PtRu catalyst, the enhancement in the PtRuRhNi catalyst should be collectively considered and the various sources of enhancement defined, i.e., the electronic and chemical states of Pt/Ru, and the chemical states of Rh/Ni. Finally, we suggest the possibility for a systematic approach to the design of novel platinum-based multimetallic alloy electrocatalyst, and those corresponding investigations are currently underway.

Acknowledgments

We acknowledge support by KOSEF through the Research Center for Energy Conversion and Storage and the Brain Korea 21 project from the Ministry of Education.

References

[1] M.P. Hearth, G.A. Hards, Platinum Met. Rev. 40 (1996) 150.
[2] A. Hamnett, Catal. Today 38 (1997) 445.
[3] E. Reddington, A. Sapienza, B. Gurau, R. Viswanathan, S. Sarangapani, E.S. Smotkin, T.E. Mallouk, Science 280 (1998) 1735.
[4] P.N. Ross, in: J. Lipkowski, P.N. Ross (Eds.), Electrocatalysis, Wiley–VCH, New York, 1998, ch. 2.
[5] A. Wieckowski (Ed.), Interfacial Electrochemistry, Dekker, New York, 1999, ch. 44–51.
[6] K.-W. Park, K.-S. Ahn, J.-H. Choi, Y.-C. Nah, Y.-E. Sung, Appl. Phys. Lett. 82 (2003) 1090.
[7] M. Watanabe, S. Motoo, J. Electroanal. Chem. 60 (1975) 275.
[8] R. Liu, H. Iddir, Q. Fan, G. Hou, A. Bo, K.L. Ley, E.S. Smotkin, Y.-E. Sung, H. Kim, S. Thomas, A. Wieckowski, J. Phys. Chem. B 104 (2000) 3518.
[9] J.B. Goodenough, R. Manoharan, A.K. Shukla, K.V. Ramesh, Chem. Mater. 1 (1989) 391.
[10] T. Toda, H. Igarashi, H. Uchida, M. Watanabe, J. Electrochem. Soc. 146 (1999) 3750.
[11] K.-W. Park, J.-H. Choi, B.-K. Kwon, S.-A. Lee, Y.-E. Sung, H.-Y. Ha, S.-A. Hong, H. Kim, A. Wieckowski, J. Phys. Chem. B 106 (2002) 1869.
[12] K.-W. Park, J.-H. Choi, Y.-E. Sung, J. Phys. Chem. B 107 (2003) 5851.
[13] B. Gurau, R. Viswanathan, R. Liu, T.J. Lafrenz, K.L. Ley, E.S. Smotkin, E. Reddington, A. Sapienza, C. Chan, T.E. Mallouk, J. Phys. Chem. B 102 (1998) 9997.
[14] K. Kinoshita, P. Stonehart, Modern Aspect of Electrochemistry, vol. 12, Plenum Press, New York, 1996.
[15] K.J. Klabunde, C. Mohs, in: L.V. Interrante, L.V. Hampden-Smith (Eds.), Chemistry of Advance Materials, Wiley–VCH, New York, 1998, ch. 3.
[16] S.-A. Lee, K.-W. Park, J.-H. Choi, B.-K. Kwon, Y.-E. Sung, J. Electrochem. Soc. 149 (2002) 1299.
[17] K.-W. Park, B.-K. Kwon, J.-H. Choi, I.-S. Park, Y.-M. Kim, Y.-E. Sung, J. Power Sources 109 (2002) 439.
[18] V. Radmilovic, H.A. Gasteiger, P.N. Ross Jr., J. Catal. 154 (1995) 98.
[19] W.E. O'Grady, P.L. Hagans, K.I. Pandya, D.L. Maricle, Langmuir 17 (2001) 3047.
[20] R.A. Lampitt, L.P.L. Carrette, M.P. Hogarth, A.E. Russell, J. Electroanal. Chem. 460 (1999) 80.
[21] S. Mukerjee, J. McBreen, J. Electroanal. Chem. 448 (1998) 163.
[22] J. McBreen, S. Mukerjee, J. Electrochem. Soc. 142 (1998) 3399.
[23] R. Viswanathan, G. Hou, R. Liu, S.R. Bare, F. Modica, G. Mickelson, C.U. Segre, N. Leyarovska, E.S. Smotkin, J. Phys. Chem. B 106 (2002) 3458.
[24] D.R. Rolison, P.L. Hangans, K.E. Swider, J.W. Long, Langmuir 15 (1999) 774.
[25] J.W. Long, R.M. Stroud, K.E. Swider-Lyons, D.R. Rolison, J. Phys. Chem. B 104 (2000) 9772.
[26] W. Dmowksi, T. Egami, K.E. Swider-Lyons, C.T. Love, D.R. Rolison, J. Phys. Chem. B 106 (2002) 12677.
[27] A.S. Arico, G. Monforte, E. Modica, P.L. Antonucci, V. Antonucci, Electrochem. Commun. 2 (2000) 466.
[28] A. Kowal, S.N. Port, R.J. Nichols, Catal. Today 38 (1997) 483.
[29] A.A. El-Shafei, J. Electroanal. Chem. 471 (1999) 89.
[30] R. Manoharan, J.B. Goodenough, J. Mater. Chem. 2 (1992) 875.